Coupling a Lattice Boltzmann and a Finite Difference Scheme

Paul Albuquerque[1,2], Davide Alemani[3], Bastien Chopard[1], and Pierre Leone[1,2]

[1] Computer Science Department, University of Geneva, 1211 Geneva 4, Switzerland
[2] LII, Ecole d'Ingénieurs de Genève, HES-SO, 1202 Geneva, Switzerland
[3] CABE, University of Geneva, 1211 Geneva 4, Switzerland

Abstract. We show how a lattice Boltzmann (LB) scheme can be spatially coupled with a finite difference (FD) scheme in order to solve the same problem. The typical situation we consider is a computational domain which is partitioned in two regions. The same spatio-temporal physical process extends over the full domain but a different numerical method is used over each region. At the interface of the subdomains, the LB and FD must be connected so as to ensure a perfect continuity of the physical quantities. We derive the theoretical concepts, which allow us to link both methods in the case of a diffusion process, and validate them with numerical simulations on a 2D domain.

1 Introduction

Many physical systems include phenomena at different time and space scales. Their description in terms of a numerical model is therefore a difficult task as often the same numerical scheme is not efficient over the full range of scales. In addition, it occurs that various physical processes take place and couple different parts of the system. Again, it is challenging to devise a numerical method which is able to efficiently deal with such constraints.

Here we consider the case of a spatially extended system in which separate spatial regions are treated with different numerical schemes. The motivation is that, depending on the nature of each region, optimal efficiency is obtained with different numerical methods.

For instance the lattice Boltzmann (LB) method [1] has a more detailed microscopic description than a finite difference (FD) scheme because the LB approach includes the molecular velocity of the particles. In addition, important physical quantities, such as the stress tensor, or particle current, are directly obtained from the local information. However, the LB scheme may require more memory than the corresponding FD scheme. Another motivation is that boundary conditions are more or less naturally imposed on a given numerical scheme. Therefore, in order to improve the global quality of the numerical solution, it may be quite efficient to assume that several solvers are coupled.

Obviously, this coupling should not produce any discontinuities at the interface between regions that are treated with the LB or the FD method. Since each

scheme uses different variables, it is crucial to understand how the LB set of variables is related to the FD set, and conversely.

Our solution follows the same argument as developed in [2] for a multigrid LB scheme: the connection between the full set of LB variables and the standard macroscopic physical quantities is based on the splitting of the particle distribution functions in an equilibrium and a nonequilibrium part. The former is built on the physical quantities and the latter on the gradient of these quantities. This observation is quite general and could be used to couple any scheme (e.g. finite volume or finite element) with any LB method. Indeed, if the two schemes use different variables, one must compute the particle distribution functions starting from physical quantities known from another solver or from an analytical expression. Here we will only consider the case of a diffusion process on a given domain which is solved by the LB approach on a chosen subdomain and with a FD solver on the rest of the domain.

Hybrid methods have already been proposed in the literature. In [3] a finite volume and a finite element method are combined and then coupled with a finite difference time domain solver for the wave equation, allowing the simulation of wave propagation in complex 3D geometry. In [4], the LB method is coupled with a molecular dynamics simulation of polymers. However, to our knowledge, the FD and LB schemes have never been coupled across adjacent regions.

The paper is organized as follows. In section 2 we briefly introduce the LB approach (we assume that the reader is familiar with the FD method). The special case of a diffusion process is discussed in section 3. In particular, it is shown how the Chapman-Enskog expansion offers a mapping between the LB variables and the macroscopic quantities and their spatial derivatives. In section 4 we describe the coupling algorithm. Then, in section 5 we perform a numerical simulation to demonstrate that the proposed coupling is correct. Finally, section 6 summarizes our findings and draws some conclusions.

2   The Lattice Boltzmann Approach

A lattice Boltzmann (LB) model [1,5] describes a physical system in terms of a mesoscopic dynamics: fictitious particles move on a regular lattice, synchronously at discrete time steps. An interaction is defined between the particles that meet simultaneously at the same lattice site. Particles obey collision rules which reproduce, in the macroscopic limit, an equation of physics.

A LB model can be interpreted as a discretization of the Boltzmann transport equation on a regular lattice of spacing Δr and with discrete time step Δt. The possible velocities for the pseudo-particles are the vectors $\boldsymbol{v}_i$. They are chosen so as to match the lattice direction: if $\boldsymbol{r}$ is a lattice site, $\boldsymbol{r} + \boldsymbol{v}_i \Delta t$ is also a lattice point. We thus consider a dynamics with $z + 1$ possible velocities, where z is the lattice coordination number and $\boldsymbol{v}_0 = 0$ describe the population of rest particles.

For isotropy reasons the lattice topology must satisfy the conditions

$$\sum_i v_{i\alpha} = 0 \quad \text{and} \quad \sum_i v_{i\alpha} v_{i\beta} = v^2 C_2 \delta_{\alpha\beta} \tag{1}$$

where C_2 is a numerical coefficient which depends on the lattice topology. The greek indices label the spatial dimensions and $v = \Delta t/\Delta r$. The first condition follows from the fact that if $\boldsymbol{v}_i$ is a possible velocity, then so is $-\boldsymbol{v}_i$.

In the LB approach a physical system is described through density distribution functions $f_i(\boldsymbol{r}, t)$. For hydrodynamics and diffusion processes, $f_i(\boldsymbol{r}, t)$ represents the distribution of particles entering site $\boldsymbol{r}$ at time t and moving in direction $\boldsymbol{v}_i$. For the wave model, the interpretation is less obvious as f_i can be positive as well as negative. Physical quantities can be defined from moments of these distributions. For instance, the local density is obtained by $\rho = \sum_{i=0}^{z} f_i$.

A LB model can be determined by specifying a lattice, a kinetic equation and an equilibrium distribution. In its simplest form (BGK model), the dynamics can be written as a relaxation to a given local equilibrium

$$f_i(\boldsymbol{r} + \boldsymbol{v}_i \Delta t, t + \Delta t) - f_i(\boldsymbol{r}, t) = \frac{1}{\tau} \left(f_i^{eq}(\boldsymbol{r}, t) - f_i(\boldsymbol{r}, t) \right) \tag{2}$$

where τ is a relaxation time, which is a free parameter of the model. The local equilibrium solution f_i^{eq} contains all the information concerning the physical process investigated. It changes according to whether we consider hydrodynamics, diffusion or wave propagation.

3   The Lattice Boltzmann Diffusion Model

Diffusion processes were first modeled using a cellular automata approach [6]. The scheme was then extended to a LB dynamics with a BGK collision term [1, 5,7].

From now on, we assume that the diffusion process takes place on a d-dimensionnal square lattice. The key point is to choose correctly the local equilibrium f_i^{eq} so that the diffusion equation for the particle density $\rho = \sum_{i=0}^{2d} f_i$ can be derived from eq. (2). Since the particle density ρ is the only conserved quantity in a diffusive process, the local equilibrium f_i^{eq} is taken to be $f_i^{eq}(\boldsymbol{r}, t) = \rho(\boldsymbol{r}, t)/2d$ so that ρ is indeed conserved and f_i^{eq} depends on $\boldsymbol{r}$ and t only through the conserved quantities [1,5].

Let us now assume that Δt is small (and constant in all our computations). Taylor expanding the left hand side of eq. (2) up to second order, we get

$$\Delta t(\boldsymbol{v}_i \cdot \nabla) f_i(\boldsymbol{r}, t) + \Delta t \, \partial_t f_i(\boldsymbol{r}, t) + \frac{\Delta t^2}{2} \partial_t^2 f_i(\boldsymbol{r}, t) +$$
$$\Delta t^2 (\boldsymbol{v}_i \cdot \nabla) \partial_t f_i(\boldsymbol{r}, t) + \frac{\Delta t^2}{2} (\boldsymbol{v}_i \cdot \nabla)^2 f_i(\boldsymbol{r}, t) = \frac{1}{\tau} \left(f_i^{eq}(\boldsymbol{r}, t) - f_i(\boldsymbol{r}, t) \right). \tag{3}$$

We then use the multiscale Chapman-Enskog expansion to solve eq. (3). Thus, we set $f_i = f_i^{(0)} + f_i^{(1)} + f_i^{(2)} + \dots$ and introduce next a small parameter ϵ along with the change of coordinates $(\boldsymbol{r}, t) \mapsto (\boldsymbol{r}_1, t_1, t_2) = (\epsilon \boldsymbol{r}, \epsilon t, \epsilon^2 t)$. We also consider a new function $f_i^\epsilon(\boldsymbol{r}_1, t_1, t_2)$ which satisfies $f_i(\boldsymbol{r}, t) = f_i^\epsilon(\epsilon \boldsymbol{r}, \epsilon t, \epsilon^2 t)$. After formally substituting $f_i \longrightarrow f_i^\epsilon$, $\nabla_r \longrightarrow \epsilon \nabla_{r_1}$, $\partial_t \longrightarrow \epsilon \partial_{t_1} + \epsilon^2 \partial_{t_2}$, into eq. (3), we obtain a new equation for f_i^ϵ.

To find an asymptotic series solution, we expand f_i^ϵ in powers of ϵ

$$f_i^\epsilon(\boldsymbol{r}_1, t_1, t_2) = f_i^{\epsilon(0)}(\boldsymbol{r}_1, t_1, t_2) + \epsilon f_i^{\epsilon(1)}(\boldsymbol{r}_1, t_1, t_2) + \epsilon^2 f_i^{\epsilon(2)}(\boldsymbol{r}_1, t_1, t_2) + \dots \quad (4)$$

By introducing (4) into the equation for f_i^ϵ, we can recursively determine the $f_i^{\epsilon(j)}$s. Using particle density conservation and the first equation in (1), we get at zero and first order

$$f_i^{(0)}(\boldsymbol{r}, t) = \frac{\rho(\boldsymbol{r}, t)}{2d} = f_i^{eq}(\boldsymbol{r}, t), \quad f_i^{(1)} = -\frac{\tau \Delta t}{2d} \boldsymbol{v}_i \cdot \nabla \rho(r, t).$$

It is still worth noticing, with respect to the macrocospic behaviour of our model, that the particle density $\rho(\boldsymbol{r}, t)$ satisfies the diffusion equation. Indeed, using the second equation in (1), we get

$$\partial_t \rho(\boldsymbol{r}, t) = \frac{C_2 v^2 \Delta t}{2d} \left(\tau - \frac{1}{2} \right) \nabla^2 \rho(\boldsymbol{r}, t),$$

with diffusion coefficient $D = (\tau - 1/2) C_2 v^2 \Delta t / (2d)$.

4   The Coupling Algorithm

The result of the previous section shows that the LB variables can be written as $f_i = f_i^{eq} + f_i^{neq}$, where

$$f_i^{eq} = f_i^{(0)} = \frac{\rho(\boldsymbol{r}, t)}{2d}, \quad f_i^{neq} \approx f_i^{(1)} = -\frac{\tau \Delta t}{2d} \boldsymbol{v}_i \cdot \nabla \rho(r, t).$$

These relations give a dictionary to go from the standard description of diffusion, where only ρ is considered, to the LB description. Note that the inverse connection is straightforward since we always have, by definition, $\rho = \sum_i f_i$. It must be clear that the LB scheme requires more information on the physical variables because it contains more degrees of freedom.

To make the coupling between a FD and a LB scheme more explicit, we now consider the situation of a two-dimensional diffusion problem $\partial_t \rho = D \nabla^2 \rho$ on a square domain $\Omega \subset \mathbb{R}^2$ of size $L_x \times L_y$. We cut Ω into two parts Ω_1 and Ω_2 such that $\Omega = \Omega_1 \bigcup \Omega_2$. We apply in Ω_1 the FD method and in Ω_2 the LB method (see fig. 1). We assume here that the same mesh is used for both methods.

We define the quantities $\boldsymbol{v}_i$, $i = 1, ..., 4$, as vectors pointing in the four lattice directions: right, up, left and down. Their lengths are such that $\boldsymbol{v}_i \Delta t$ connects the neighboring sites along direction i.

For the points $\boldsymbol{r} \in \Omega_1$, we apply the FD scheme to the diffusion equation

$$\rho(\boldsymbol{r}, t + \Delta t) = \rho(\boldsymbol{r}, t) + \frac{\Delta t}{\Delta r^2} D \sum_{i=1}^{4} \left(\rho(\boldsymbol{r} + \boldsymbol{v}_i \Delta t, t) - \rho(\boldsymbol{r}, t) \right), \quad (5)$$

whereas the points $\boldsymbol{r} \in \Omega_2$ are treated with the LB scheme given by eq. (2). There are several ways to define the interface between the two regions, Ω_1 and
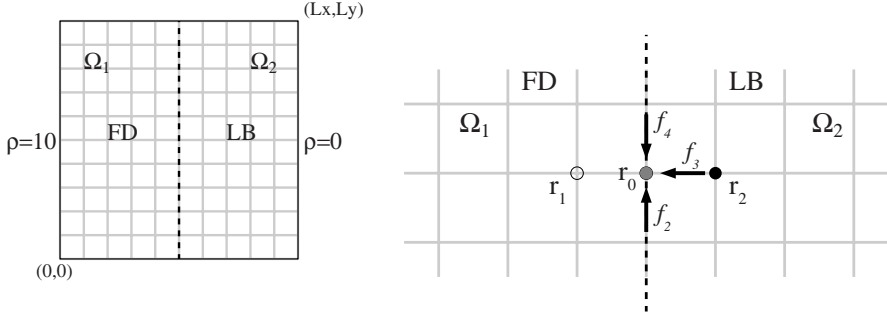
Fig. 1. Left: The computational grid and its partioning into a subdomain Ω_1, where the FD scheme is applied, and a subdomain Ω_2, where the LB scheme is used. The boundary conditions we impose for the diffusion process are $\rho = 10$ on the left wall, $\rho = 0$ on the right one and periodic along the vertical axis. Right: The point r_1 (white circle), resp. r_2 (black circle), is completely treated with the FD, resp. LB, scheme, and r_0 (gray circle) is updated with both methods. The figure shows that for r_0, the distribution f_1 is unknown (because it should come out of r_1). Thus, we use our coupling algorithm to compute it

Ω_2. Here, we assume an overlap so that a point r_0 at the interface belongs to both Ω_1 and Ω_2 (see fig. 1). On such points r_0, the LB variables as well as the FD variables are computed. We denote by $r_1 \in \Omega_1$ and $r_2 \in \Omega_2$, two neighbors of a site r_0 of the interface. According to fig. 1 and eq. (5), the calculation of $\rho(r_0, t + \Delta t)$ requires the knowledge of $\rho(r_2, t)$, where r_2 is only subject to the LB scheme. However, the LB scheme offers naturally this quantity as $\rho(r_2, t) = \sum_{i=1}^{4} f_i(r_2, t)$. Therefore, the coupling of a FD site to a LB site is straightforward. The reverse is a bit more involved. In order to update the LB scheme at r_0 and time $t + \Delta t$, we need $f_1(r_0, t)$. This quantity is not known because the site r_1 is only treated with the FD scheme. Indeed, if the LB scheme had been applied to the full domain, then $f_1(r_0, t)$ would have been propagated from lattice site r_1. However, the value of $f_1(r_0, t)$ can be computed from our dictionary $f_1(r_0, t) = f_1^{(0)}(r_0, t) + f_1^{(1)}(r_0, t)$ with $f_1^{(0)}(r_0, t) = \rho(r_0, t)/4$ and $f_1^{(1)}(r_0, t) = -(\tau \Delta t/4)\, v_i \cdot \nabla \rho(r_0, t)$. In order to obtain $\nabla \rho(r_0, t)$, we use a second order finite difference approximation of ρ over the nearest neighbors

$$\nabla \rho(r_0, t) = \frac{\rho(r_2, t) - \rho(r_1, t)}{2 \Delta r}. \tag{6}$$

Note that in the particular case where only one f_i is missing, the connection can be made in a simpler way. As $\rho = \sum_i f_i$ is known from the FD calculation, and f_2, f_3 and f_4 are known from the LB calculation, one has $f_1 = \rho - f_2 - f_3 - f_4$. In the simple case described here, this approach gives a correct coupling. However, it no longer works if the interface between Ω_1 and Ω_2 is irregular because the previous expression is not sufficient to determine more than one f_i.

5   Numerical Validation

To validate the coupling algorithm proposed in the previous section, we performed the simulation of a source-sink problem on the geometry defined in fig. 1. The domain size is $L_x = L_y = 30$ in lattice units. The boundary conditions are $\rho((0, y), t) = 10$ and $\rho((L_x, y), t) = 0$ on the left and right sides of Ω and the initial conditions are $\rho((0, y), 0) = 10$ and $\rho((x, y), 0) = 0$ for $x \neq 0$. On the lower and upper walls, we apply periodic conditions $\rho((x, L_y + 1), t) = \rho((x, 0), t)$ and $\rho((x, -1), t) = \rho((x, L_y), t)$. The vertical interface between the subdomains is positioned at $x = 6$, with the FD scheme over the left region and the LB over the right one. Hence, the geometry is actually 1-dimensional.

This simple set-up with the above boundary and initial conditions allows for an analytic solution to the diffusion equation for the time-dependent dynamics,

$$\rho((x, y), t) = \rho_0 \sum_{i=0}^{\infty} \mathrm{erfc} \left(\frac{L_x(1 - (1 - x/L_x) + 2i)}{2\sqrt{Dt}} \right)$$
$$- \rho_0 \sum_{i=0}^{\infty} \mathrm{erfc} \left(\frac{L_x(1 - (1 + x/L_x) + 2i)}{2\sqrt{Dt}} \right)$$

where $\mathrm{erfc}(v) = \int_v^{\infty} e^{-u^2} du$ and D is the diffusion coefficient (here $\rho_0 = 10$).

After several iterations, the system converges to a steady state in which the density profile is expected to be a linear function of x satisfying the boundary conditions. To illustrate the importance of a correct coupling at the subdomain interface, we plot in figs. 2a, 2b, 2c (left) the density profile obtained from the numerical solution with the full coupling $f_1 = f_1^{(0)} + f_1^{(1)}$, the one without the gradient correction, i.e. with the approximation $f_1 \approx f_1^{(0)}$, and the theoretical profile. We also plot in figs. 2a, 2b, 2c (right) the error with respect to the analytic solution. From the breaking of the slope observed in fig. 2c (left) we conclude that the gradient correction is necessary to obtain the correct density profile and continuity of the particle current.

We computed the relative error in the L^2-norm for the lattice resolution used in the simulation. For 100 (resp. 500, 5000) time steps, we get a 1.2% (resp. 0.6%, 0.3%) relative error for the full coupling. We expect the level of accuracy of our mapping to be the same as the LB itself: second order in the lattice spacing.

6   Conclusion

In this work, a LB scheme is spatially coupled to a FD scheme on a computational domain partitioned in two regions. We propose a way to relate the LB distribution functions f_i with the classical physical quantities and their derivatives. This is a first step towards coupling correctly a LB scheme with another method. Hence, to focus on the methodology only, we consider the simplest possible situation: a diffusion process solved by the LB approach on one region and
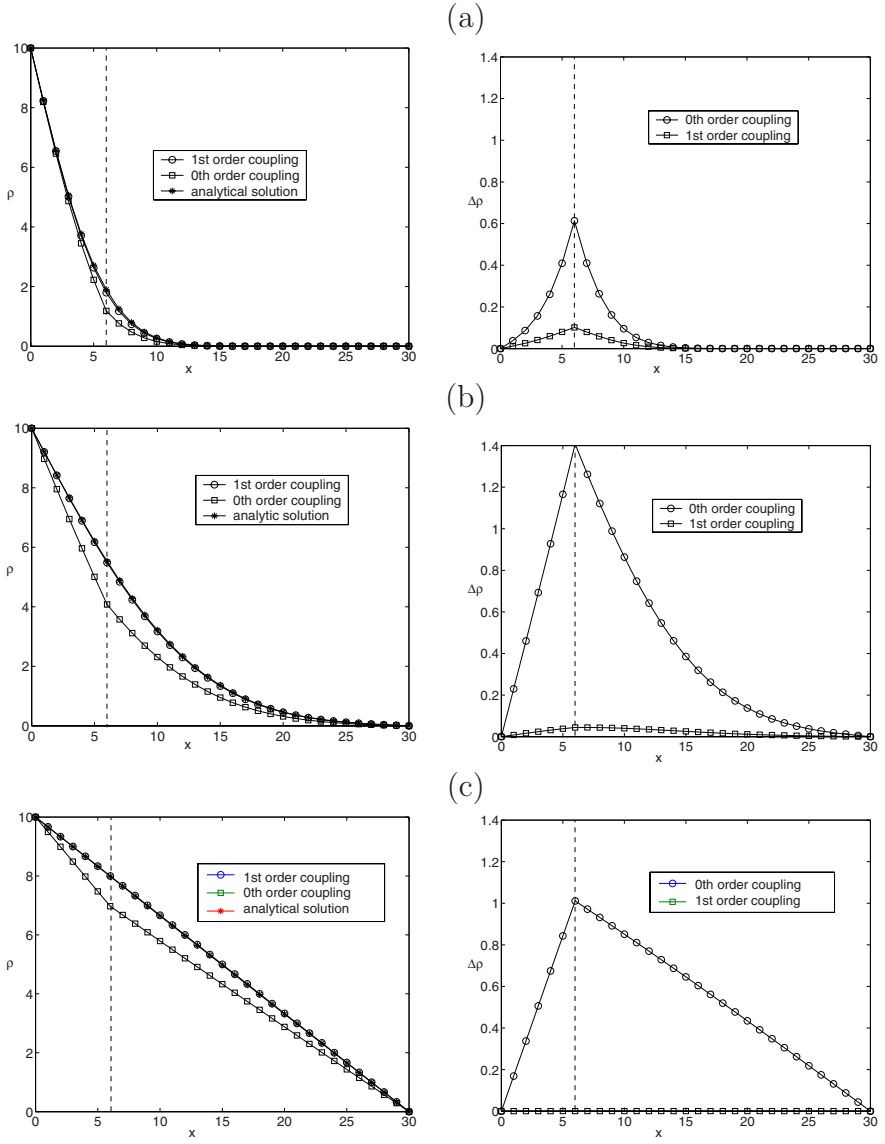
Fig. 2. The density profile along the horizontal axis of the domain Ω is plotted on the left side and the error with respect to the analytic solution on the right side. The squares correspond to a simulation in which the coupling algorithm does not include the gradient correction, whereas the circles represent the case where the full coupling is considered. The asterisks of the analytic solution are diffcult to distinguish from the circles of the full coupling. The total grid size is 31×31, and there are respectively (a)100, (b)500 and (c)5000 time steps. The vertical interface (dashed line) is located at $x = 6$. The relaxation time is $\tau = 0.7$, the lattice spacing $\Delta r = 1$ and the time step $\Delta t = 10^{-1}$

with a FD solver on the other. At the interface, the LB and FD are connected so as to preserve continuity of the physical quantities. The connection between the f_is and the standard macroscopic physical quantities is obtained using a multiscale Chapman-Enskog expansion to split the f_is in an equilibrium and a nonequilibrium part. The former is related to the particle density and the latter to its gradient. Our coupling methodology is indeed an approximation since we neglect higher-order derivatives in the nonequilibrium distributions. A validation was performed by running numerical simulations on a 2D domain and comparing them with an analytic solution. Our mapping has the same level of accuracy as the LB itself: second order in the lattice spacing.

Regarding future work, it seems natural to try to couple two domains with different meshes. A good enough interpolation is needed to keep the second-order accuracy of the coupling scheme (see [2]). This as well as the case of an irregular boundary is under investigation. Other perspectives include applying the same methodology to the LB reaction-diffusion, wave and fluid models. We also wish to couple different LB dynamics: a diffusive region with a convective one. With respect to coupling an incompressible Navier-Stokes solver with a "compressible" LB fluid model, we believe that the pressure obtained from the Navier-Stokes solver can be used to specify the density of the LB scheme, and conversely. We plan to examine this on a Poiseuille flow and on Blasius' problem.

References

1. B. Chopard, P.O. Luthi, A. Masselot, and A. Dupuis. Cellular automata and lattice Boltzmann techniques: An approach to model and simulate complex systems. *Advances in Complex Systems*, 5(2), 2002.
   http://cui.unige.ch/~chopard/FTP/CA/advp.ps.gz.
2. A. Dupuis and B. Chopard. Theory and applications of alternative lattice Boltzmann refinement algorithm. *Phys. Rev. E*, 67:066707, 2003. In press.
3. L. Beilina. A hybrid method for elastic waves. Technical report, Finite Element Center, Chalmers University of Technology, 2003. Preprint 2003-01.
4. A. Malevanets and R. Kapral. Mesoscopic model for solvent dynamics. *J. of Chem. Phys.*, 110(17):8605–8613, May 1999.
5. D.A. Wolf-Gladrow. *Lattice-Gas Cellular Automata and Lattice Boltzmann Models: an Introduction*. LNM, 1725. Springer, Berlin, 2000.
6. B. Chopard and M. Droz. Cellular automata model for diffusion processes. *J. Stat. Phys.*, 64:859–892, 1991.
7. R. G. M. Van der Sman and M. H. Ernst. Convection-diffusion lattice boltzmann scheme for irregular lattices. *J. Comp. Phys.*, 160:766–782, 2000.